Since January 2020 Elsevier has created a COVID-19 resource centre with free information in English and Mandarin on the novel coronavirus COVID-19. The COVID-19 resource centre is hosted on Elsevier Connect, the company's public news and information website.

Biomedical Signal Processing and Control 79 (2023) 104107

Contents lists available at ScienceDirect

Biomedical Signal Processing and Control

journal homepage: www.elsevier.com/locate/bspc

Multi-objective T-S fuzzy control of Covid-19 spread model: An LMI approach

Reza Najarzadeh [a], Mohammad Hassan Asemani [a,*], Maryam Dehghani [a], Mokhtar Shasadeghi [b]

[a] School of Electrical and Computer Engineering, Shiraz University, Shiraz, Iran
[b] Department of Electrical and Electronics Engineering, Shiraz University of Technology, Shiraz, Iran

ARTICLE INFO

Keywords:
Covid 19 model
Robust T-S fuzzy controller
Linear matrix inequalities (LMIs)
Multi objective controller

ABSTRACT

Due to the importance of control actions in spreading coronavirus disease, this paper is devoted to first modeling and then proposing an appropriate controller for this model. In the modeling procedure, we used a nonlinear mathematical model for the covid-19 outbreak to form a T-S fuzzy model. Then, for proposing the suitable controller, multiple optimization techniques including Linear Quadratic Regulator (LQR) and mixed $H_2 - H_\infty$ are taken into account. The mentioned controller is chosen because the model of corona-virus spread is not only full of disturbances like a sudden increase in infected people, but also noises such as unavailability of the exact number of each compartment. The controller is simulated accordingly to validate the results of mathematical calculations, and a comparative analysis is presented to investigate the different situations of the problem. Comparing the results of controlled and uncontrolled situations, it can be observed that we can tackle the devastating hazards of the covid-19 outbreak effectively if the suggested approaches and policies of controlling interventions are executed, appropriately.

1. Introduction

These days, almost all countries worldwide are struggling with coronavirus and the challenges it creates. Each country's government should take suitable actions in two aspects. First, the decision-makers should specify an organized policy for measures like restriction, lock-down, social distancing, and vaccination to prevent the spread of coronavirus and secure the population [1]. Second, the resources for pharmaceutical and non-pharmaceutical measures like face masks, ventilators, hospital beds, medicines, and vaccines should be provided.

The virus named SARS-coV-2 was discovered in the province of Wuhan in China on December 31, 2019 [2]. The disease was highly like influenza and entangled the body's respiratory system. The primary way of transmission of the virus is the aerosols. So, the direct method to prevent the virus from spreading and making the people infected is to use face masks [2]. Besides, the data of the countries that started vaccination months ago and vaccinated a considerable proportion of their people show us that vaccination is an excellent and practical way of dealing with the disease [3,4].

The studies and the statistics declared that vaccinated individuals are much more secure than unvaccinated ones from getting hospitalized and dying due to the covid-19 [5]. Nevertheless, based on prior knowledge of epidemiology, we know that almost 70 to 80 percent of the population should be immune to the disease by getting vaccinated or being infected and then recovered, leading to herd immunity [6]. The exact number of people who need to be immune to the disease to reach herd immunity depends on many factors like age groups and the disease's contagiousness. The disease symptoms remain latent for about 2–14 days during the incubation period, and after that, there would be some severe or mild symptoms like sneezing, headache, tiredness, and coughing [7]. There might be a possibility that the infected person does not show any symptoms, so they can transmit the virus to others even without knowing that they were infected. There are more than 549 million total infected cases and more than 6 million deceased cases of covid-19 globally, which makes it one of the world's most significant epidemic diseases [8]. The number of infected patients might even be more than this, because based on World Health Organization (WHO) reports, the number of covid-19 tests is enough to show a high proportion of infected individuals if the positive tests were not be more than 10% out of all taken tests [9].

A factor shows the contagiousness of the disease known as reproduction number or $\mathscr{R}_0$ [10]. A mathematical procedure can obtain this

* Corresponding author.
E-mail address: asemani@shirazu.ac.ir (M.H. Asemani).

https://doi.org/10.1016/j.bspc.2022.104107
Received 1 May 2022; Received in revised form 12 August 2022; Accepted 15 August 2022
Available online 18 August 2022

term on the model of the disease. One of its importance is that the policymaker could relax or tighten the restrictions and lockdowns in society based on this term. They can ease the restrictions if the reproduction number value is less than one. However, the situation should be stricter if the term's value is more than one.

The process of recognizing different diseases and disorders is done by using detection methods, where one of the most impactful methods is computer-aided diagnosis algorithms [11,12]. After recognizing the illness, the process of controlling covid-19 spread is started. For this purpose, a proper mathematical model is needed to include both general and specific aspects of the patients [13]. The basic model for the epidemic disease is Susceptible-Infected-Recovered (SIR) compartmental model [14]. The more detailed the model is, the more one learns about the system's behavior [1,14–21]. Several models have been developed for the covid-19 epidemic recently. A Susceptible-Probable-Infected-Recovered (SPIR) model was developed to study and forecast the behavior of covid-19 in the West Java province of Indonesia and Michigan in the USA [22]. Then, the time-varying reproduction number was estimated based on EKF (extended Kalman filter). It was shown that the value of the reproduction number might be higher considering the probable cases. In [23], a Susceptible-Infected-Recovered-Virus density (SIRV) model was used to show the effects of the virus on susceptible persons. A comparison between the actual data of India and the proposed model declared the efficacy of the model. The effectiveness of restrictive measures in society has been studied through the model details. In [16], a data-driven Susceptible-Infected-Recovered- Deceased (SIRD) model is proposed and tested by actual data. Moreover, a nonlinear model predictive control is taken into account so that a decent strategy could be made to lower the catastrophic effects of the coronavirus. In this model, the parameters are time-varying and are updated every week. So, the decision-makers can reappraise the controlling measures every week. It shows that the number of dead people could be lowered to 30 percent using the suggested controller design. In [24], a Susceptible-Infected-Recovered (SIR) and a Susceptible-Infected-Recovered-Quarantined (SIRQ) model are proposed, and the variation of the parameters are studied to understand the effects of different factors on the virus spread better such as virus mutation, lockdown and holding events. A Susceptible-Exposed-Quarantined-Infected-Recovered (SEQIR) model has been used, reducing the spread of the virus and its harmful effects on the economy [18]. Then, a policy for restriction is made by combining the U-model controller and extended state observer. Two examples compare the controller performance with linear active disturbance rejection control. The study results state that the first controller (U-model controller) has a more feasible response for the control problem. A Susceptible-Exposed-Quarantined-Infected-Hospitalized-Recovered (SEQIHR) model is developed to help governments find the best strategy to cope with covid-19 challenges [15]. Accordingly, the nonlinear least square method estimates the value of the nonlinear model parameters.

This paper applies a nonlinear SIRQ model of covid-19 to extract the Takagi-Sugeno (T-S) fuzzy model. The reproduction number is calculated using the next-generation matrix approach. Then, the stability of the proposed model is guaranteed using a feedback controller design. The controller is designed based on an optimization problem to minimize a unified optimization problem, resulting in robust optimal stabilizing control with proper performance. The stability problem is solved by turning the stability and performance condition into some Linear Matrix Inequalities (LMIs). It will be seen that the proposed controller is robust against the uncertainties and the external disturbances. The simulation results will suggest strategies such as rate of vaccination and hospitalization and a lockdown policy to control the covid-19 outbreak. The proposed method acts better than the robust Linear Parameter Varying (LPV) controller proposed in [25] since it seeks the optimum result of dealing with the covid-19 model with minimum control effort and mathematical calculation. As the natural system consists of both uncertainties and nonlinearities, working on this method helps us consider and get more realistic results from our simulation.

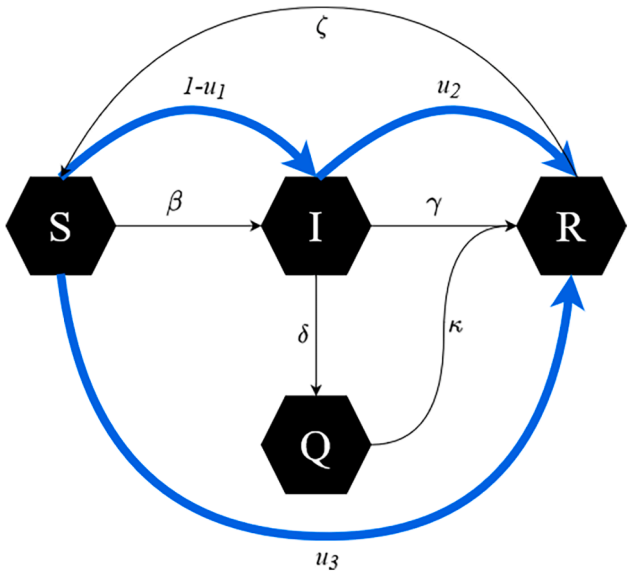

Fig. 1. The schematic of covid-19 nonlinear model with four states as S(susceptible), I (infected), R (recovered), and Q (quarantined) parts and three control inputs as u_1 (social distancing and lockdown), u_2 (treatments), and u_3 (vaccination).

This paper is organized as follows: the nonlinear model of covid-19 is presented in Section 2. In Section 3, the T-S fuzzy model is formed, and the controller design procedure and stability conditions are presented. Section 4 shows the simulation results of applying the robust controller to the model. The final section, Section 5, makes some conclusions about the study, and some future works are suggested. Choosing the best strategy to face the covid-19 issue is discussed, too.

2. Dynamic model of covid-19

2.1. Nonlinear model of covid-19

In this work, a SIRQ covid-19 model is considered [24,26]. The model is also modified to have a more realistic sense. It can be noted that any other model which meets the necessary mathematical conditions can be used alternatively without any problems, and we just used this model to verify the efficiency of the proposed approach. As shown in Fig. 1, this model consists of four state variables showing susceptible, infected, recovered (or immunized), and quarantined individuals, respectively. There are three control inputs for the proposed model, which are u_1 (social distancing and lockdown), u_2 (treatments), and u_3 (vaccination). The mathematical model of SIRQ is given in (1).

$$\dot{x} = f(x(t)) = \begin{cases} \dot{S}(t) = -\beta\dfrac{S(t)I(t)}{N}(1-u_1(t)) + \zeta R(t) - u_3(t)S(t) \\ \dot{I}(t) = \beta\dfrac{S(t)I(t)}{N}(1-u_1(t)) - \gamma I(t) - \delta I(t) - u_2(t)I(t) \\ \dot{R}(t) = \gamma I(t) - \zeta R(t) + \kappa Q(t) + u_3(t)S(t) + u_2(t)I(t) \\ \dot{Q}(t) = \delta I(t) - \kappa Q(t) \end{cases} \tag{1}$$

where $x(t) = [S(t) \quad I(t) \quad R(t) \quad Q(t)]^T$ are the states of the model. Model (1) is built based on the following propositions:

- People leave susceptible compartment to infected compartment at rate β, while control input u_1 shows the contact rate decrement of susceptible and infected individuals. Larger u_1 values will result in a lower transmission rate from the susceptible to the infected

compartment. Susceptible individuals could also be immune to the disease by getting vaccinated with the u_3 rate. The parameter ζ also considers the possibility of immunized compartment reinfection.
- Infected people move to quarantined part with a rate of δ. The input control u_2 is the rate of medical care and treatment, which secure infected people. The infected people also go to the immunized compartment at the rate of γ.
- The people in quarantined section can move to immunized compartment at the rate of κ.
- $N = S + I + R + Q$ where N shows the population of the society.
- We also added the deceased cases to our analysis as an output $D = \sigma I$ for the T-S fuzzy system. Based on the coronavirus statistics [8], the parameter σ is estimated to be equal to be $\sigma = 0.0112$.

This model can show the behavior of the coronavirus epidemic to some good point. It can be noted that the control input for this system should be in the bound [0,1], because a normalized controller values in the simulation, gives the reader a better sense of the subject. However, in the real world, there are even more restrictions on control input values than this. As it is impossible to use the maximum capacity of the control measures, the values of control inputs should be as small as possible, and we tried to implement this factor in this paper. The system's initial condition has to be non-negative because the system is inherently positive.

2.2. Reproduction number

We are going to calculate the reproduction number based on the next-generation method [27]. The disease-free equilibrium (DFE) point for this model is given by $x_0(S^*, I^*, R^*, Q^*) = (S_0, 0, 0, 0)$. Next, we define $\mathscr{F}$ from the transmission terms of the model and $\mathscr{V}$ from the infected compartments I, Q of the model as:

$$F = \begin{bmatrix} -\beta\dfrac{SI}{N} \\ \beta\dfrac{SI}{N} \\ 0 \\ 0 \end{bmatrix}, V = \begin{bmatrix} -\zeta R \\ \gamma I + \delta I \\ -\gamma I + \zeta R - \kappa Q \\ -\delta I + \kappa Q \end{bmatrix} \tag{2}$$

Then, we partitioned the model into two parts where the infected states are placed in V matrix as $(I, Q) = (x_1, x_2)$, and the other states $(S, R) = (x_1, x_2)$ are set to be in F matrix and can be specified as:

$$F = \frac{\partial \mathscr{F}_i}{\partial x_i}(x_0), V = \frac{\partial \mathscr{V}_i}{\partial x_i}(x_0); (i = 1, 2)$$

$$F \cong \begin{bmatrix} \beta & 0 \\ 0 & 0 \end{bmatrix}, V = \begin{bmatrix} \gamma + \delta & 0 \\ -\delta & \kappa \end{bmatrix} \tag{3}$$

The inverse of V is given by.

$$V^{-1} = \frac{1}{\kappa(\gamma + \delta)} \begin{bmatrix} \kappa & 0 \\ \delta & \gamma + \delta \end{bmatrix}$$
$$F^* V^{-1} = \frac{1}{\kappa(\gamma + \delta)} \begin{bmatrix} \beta\kappa & 0 \\ 0 & 0 \end{bmatrix} \tag{4}$$

Where $F^* V^{-1}$ is the so-called next-generation matrix. The basic reproduction number is achieved by [27]:

$$\mathscr{R}_0 = \rho\left(F^* V^{-1}\right) = \frac{\beta}{(\gamma + \delta)} \tag{5}$$

where ρ is the spectral radius of the next-generation matrix, called the greatest matrix eigenvalue.

The basic reproduction number's sensitivity analysis could be done using the following formulas [15]:

$$S_\beta^{\mathscr{R}_0} = \frac{\partial \mathscr{R}_0}{\partial \beta}\frac{\beta}{\mathscr{R}_0} = 1, \quad S_\delta^{\mathscr{R}_0} = \frac{\partial \mathscr{R}_0}{\partial \delta}\frac{\delta}{\mathscr{R}_0} = \frac{-\delta}{\gamma + \delta}$$

$$S_\gamma^{\mathscr{R}_0} = \frac{\partial \mathscr{R}_0}{\partial \gamma}\frac{\gamma}{\mathscr{R}_0} = \frac{-1}{\gamma + \delta} \tag{6}$$

Each sensitivity index represents how and at what rate the parameter variation affects the value of a varying quantity which is $\mathscr{R}_0$, here.

There is another index called effective reproduction number $\mathscr{R}_t$ that indicates the average number of secondary cases caused by every infectious case when we consider both susceptible and insusceptible cases in the population. The effective reproduction number also can be achieved as:

$$\mathscr{R}_t = x\mathscr{R}_0 \tag{7}$$

where x is the proportion of the host population that are susceptible.

3. T-S Fuzzy modelling and controller design

3.1. T-S Fuzzy model

In this section, the T-S fuzzy model is obtained using (1). We assume that (1) could be written as $\dot{x} = f(x(t))$ to start this procedure. Then, converting the nonlinear system into T-S fuzzy form [28,29] with affined parameters will lead to:

$$\dot{x} = f(x(t)) = \sum_{i=1}^{N_1} \rho_i(\theta) A_i x(t) + \sum_{i=1}^{N_1} \rho_i(\theta) B_i u(t); x = [S\ I\ R\ Q]^T \tag{8}$$

where N_1 is the number of T-S fuzzy model vertices in its uncertain space.

Assuming uncertainties in the parameters, the T-S fuzzy model could also be represented as follows:

$$\dot{x} = \sum_{i=1}^{N_1} \rho_i(\theta)(\widetilde{\mathrm{A}}_\mathrm{i} + \Delta\widetilde{\mathrm{A}}_\mathrm{i})x(t) + \sum_{j=1}^{N_1} \rho_i(\theta)(\widetilde{\mathrm{B}}_\mathrm{i} + \Delta\widetilde{\mathrm{B}}_\mathrm{i})u(t) \tag{9}$$

In (9), the time-varying parameters, nonlinearities, and uncertainties of A, B, and C matrices are divided into two parts. The varying parameters are assigned to $\widetilde{A}_i, \widetilde{B}_i, \widetilde{C}_i$ matrices and the uncertain parameters are assigned to $\Delta\widetilde{A}_i, \Delta\widetilde{B}_i, \Delta\widetilde{C}_i$ matrices. The decision of which parameters will be chosen in any parts of the T-S fuzzy model depends on our prior knowledge of the system and the behavior under different circumstances. This process allows us to solve the problem with less computational burden by reducing the number of vertices of the T-S fuzzy model. For instance, we know that the parameter β or transmission rate in the covid-19 model is one of the varying parameters that may vary during the time of covid-19 spread. So, this parameter should be one of the choices for the $\widetilde{A}_i$ matrix. We decided to consider all the nonlinearities of the covid-19 model in $\widetilde{A}_i, \widetilde{B}_i, \widetilde{C}_i$ matrices to understand the system's behavior better. On the other hand, the uncertain parameters are considered in $\Delta\widetilde{A}_i, \Delta\widetilde{B}_i, \Delta\widetilde{C}_i$ matrices and are supposed to be bounded in a pre-specified bound.

For model (1), the T-S fuzzy model matrices (8) could be rewritten as:

$$\widetilde{A} = \begin{bmatrix} -l_1 & -l_2 & \zeta & 0 \\ l_1 & l_2 - \delta & 0 & 0 \\ 0 & 0 & -\zeta & \kappa \\ 0 & \delta & 0 & -\kappa \end{bmatrix}, \widetilde{B} = \begin{bmatrix} l_3 & 0 & 0 \\ -l_3 & 0 & 0 \\ 0 & 0 & 0 \\ 0 & 0 & 0 \end{bmatrix}$$

$$\Delta\widetilde{A} = \begin{bmatrix} 0 & 0 & 0 & 0 \\ 0 & -\gamma & 0 & 0 \\ 0 & \gamma & 0 & 0 \\ 0 & 0 & 0 & 0 \end{bmatrix}, \Delta\widetilde{B} = \begin{bmatrix} 0 & 0 & -S \\ 0 & -I & 0 \\ 0 & I & S \\ 0 & 0 & 0 \end{bmatrix} \tag{10}$$

where $l_1 = \beta\frac{I(t)}{2N}$, $l_2 = \beta\frac{S(t)}{2N}$, $l_3 = \beta\frac{S(t)I(t)}{N}$. In the A matrix,γ, δ, l_1, l_2 are chosen as the varying parameters, and γ is chosen as uncertainty. Also, for B matrix, l_3 is chosen to be the varying parameter, while the effects of S and I parameters can be seen in the l_1 and l_2 parameters. The above matrices have many zero entries making them ill-conditioned and may result in an infeasible solution for the problem. So, we change the notation of our problem as every parameter in $\Delta\widetilde{A}_i, \Delta\widetilde{B}_i$ matrices in (10) be written such as $\gamma = \widehat{\gamma} + \Delta\gamma$ where $\widehat{\gamma}$ is the parameter's nominal value. Therefore, (10) is rephrased as:

$$\widetilde{A} = \begin{bmatrix} -l_1 & -l_2 & \zeta & 0 \\ l_1 & l_2 - \widehat{\gamma} - \delta & 0 & 0 \\ 0 & \widehat{\gamma} & -\zeta & \kappa \\ 0 & \delta & 0 & -\kappa \end{bmatrix}$$

$$\widetilde{B} = \begin{bmatrix} l_3 & 0 & -\widehat{S} \\ -l_3 & -\widehat{I} & 0 \\ 0 & \widehat{I} & \widehat{S} \\ 0 & 0 & 0 \end{bmatrix}$$

$$\Delta\widetilde{A} = \begin{bmatrix} 0 & 0 & 0 & 0 \\ 0 & -\Delta\gamma & 0 & 0 \\ 0 & \Delta\gamma & 0 & 0 \\ 0 & 0 & 0 & 0 \end{bmatrix}, \Delta\widetilde{B} = \begin{bmatrix} 0 & 0 & -\Delta S \\ 0 & -\Delta I & 0 \\ 0 & \Delta I & \Delta S \\ 0 & 0 & 0 \end{bmatrix} \tag{11}$$

The premise variables for every uncertain or varying parameter of the T-S fuzzy model in the above matrices are derived in the following form by use of the sector nonlinearity approach [25]:

$$\begin{aligned} &\delta = \theta_1\overline{\delta} + \theta_2\delta \quad ,\theta_1 + \theta_2 = 1 \quad ,\theta_1 = \frac{\overline{\delta} - \delta(t)}{\overline{\delta} - \delta} \quad ,\theta_2 = \frac{\delta(t) - \delta}{\overline{\delta} - \delta} \\ &l_1 = \theta_3\overline{l_1} + \theta_4 l_1 \quad ,\theta_3 + \theta_4 = 1 \quad ,\theta_3 = \frac{\overline{l_1} - l_1(t)}{\overline{l_1} - l_1} \quad ,\theta_4 = \frac{l_1(t) - l_1}{\overline{l_1} - l_1} \\ &l_2 = \theta_5\overline{l_2} + \theta_6 l_2 \quad ,\theta_5 + \theta_6 = 1 \quad ,\theta_5 = \frac{\overline{l_2} - l_2(t)}{\overline{l_2} - l_2} \quad ,\theta_6 = \frac{l_2(t) - l_2}{\overline{l_2} - l_2} \\ &l_3 = \theta_7\overline{l_3} + \theta_8 l_3 \quad ,\theta_7 + \theta_8 = 1 \quad ,\theta_7 = \frac{\overline{l_3} - l_3(t)}{\overline{l_3} - l_3} \quad ,\theta_8 = \frac{l_3(t) - l_3}{\overline{l_3} - l_3} \end{aligned} \tag{12}$$

where $\delta(t), l_1(t), l_2(t)$and $l_3(t)$ are the parameters' values at time t based on their variation profile.

The normalized weighted membership functions $\rho_i(\theta)$ for (i = 1,..,16) satisfy $\sum_{i=1}^{16}\rho_i(\theta) = 1$, and are obtained as:

Using the fact that $\Delta\widetilde{A}_i, \Delta\widetilde{B}_i$ matrices are bounded uncertainties, they can be re-parametrized with:

$$\begin{cases} \rho_1(\theta) = \theta_1{}^*\theta_3{}^*\theta_5{}^*\theta_7 \\ \rho_2(\theta) = \theta_1{}^*\theta_3{}^*\theta_5{}^*\theta_8 \\ \quad\vdots \\ \rho_{16}(\theta) = \theta_2{}^*\theta_4{}^*\theta_6{}^*\theta_8 \end{cases} \tag{13}$$

$$\begin{cases} \Delta\widetilde{A}_i = E_A\Delta_A(t)F_A, {\Delta_A}^T\Delta_A < I \\ \Delta\widetilde{B}_i = E_B\Delta_B(t)F_B, {\Delta_B}^T\Delta_B < I \end{cases} \tag{14}$$

where $\Delta_A(t), \Delta_B(t) \in \mathscr{R}^{n^*n}$ are the bounded uncertain matrices, and n is the number of uncertainties in each matrix. E_A, E_B, F_A, F_B are constant matrices with compatible dimensions. The matrices mentioned above for model (11) are calculated as follows:

$$E_A = \begin{bmatrix} 0 \\ -1 \\ 1 \\ 0 \end{bmatrix}, \Delta_A(t) = \Delta\gamma, F_A = [0 \quad 1 \quad 0 \quad 0]$$

$$E_B = \begin{bmatrix} -1 & 0 \\ 0 & -1 \\ 1 & 1 \\ 0 & 0 \end{bmatrix}, \Delta_B(t) = \begin{bmatrix} \Delta S & 0 \\ 0 & \Delta I \end{bmatrix}, F_B = \begin{bmatrix} 0 & 0 & 1 \\ 0 & 1 & 0 \end{bmatrix} \tag{15}$$

Having the condition that $\Delta A^{T*}\Delta A \le I$ and $\Delta B^{T*}\Delta B \le I$, (15) could be rewritten as:

$$E_A = \Delta\gamma\begin{bmatrix} 0 \\ -1 \\ 1 \\ 0 \end{bmatrix}, \Delta_A(t) = \frac{1}{\Delta\gamma}, F_A = [0 \quad 1 \quad 0 \quad 0]$$

$$E_B = (\Delta S + \Delta I)\begin{bmatrix} -1 & 0 \\ 0 & -1 \\ 1 & 1 \\ 0 & 0 \end{bmatrix}, \Delta_B(t) = \begin{bmatrix} \frac{1}{\Delta S} & 0 \\ 0 & \frac{1}{\Delta I} \end{bmatrix}, F_B = \begin{bmatrix} 0 & 0 & 1 \\ 0 & 1 & 0 \end{bmatrix} \tag{16}$$

Knowing that $N_1 = 2^4$, and concerning (9) and (16), the T-S fuzzy model will be finalized, such as:

$$\dot{x} = \sum_{i=1}^{16}\rho_i(\theta)\left(\widetilde{A}_i(t) + E_A\Delta_A(t)F_A\right)x(t) + \sum_{j=1}^{16}\rho_i(\theta)\left(\widetilde{B}_i + E_B\Delta_B(t)F_B\right)u(t) \tag{17}$$

Although, the basic T-S fuzzy model (8) consist of 7 uncertainties or varying parameters in A and B matrices, applying (14) to the system model in (9), three of the uncertainties are moved to the $\Delta\widetilde{A}_i$ and $\Delta\widetilde{B}_i$ part, and since they are considered bounded, they are removed from the uncertain space of T-S fuzzy model. Thus, the number of uncertainties in the final model in (17) is reduced to four and consequently, the number of vertices in uncertain space is 2^4. Therefore, in the case of designing a controller for the T-S fuzzy model, it is much easier to solve the problem with the modified T-S fuzzy model instead of its basic model because the uncertain space of the model has fewer vertices to check for approving its stability in the first case. This approach is advantageous for analyzing large-scale systems containing great amounts of uncertainties, varying parameters, and nonlinearities for their robust stability and performance by reducing their uncertain space vertices.

3.2. T-S Fuzzy controller design and stability analysis

In the previous subsection, we derived the T-S fuzzy model (17). Now, we are ready to start designing the controller for the system. The chosen controller here is the state feedback controller. By applying this controller on the T-S fuzzy model, it works as a robust controller that guarantees the system's stability on every vertex of the uncertain space. Using the feedback controller law of the parallel distributed control (PDC) form $u = \sum_{j=1}^{16}\rho_j(\theta)K_jx$, the closed-loop control system is described as:

$$\dot{x} = \sum_{i=1}^{16}\sum_{j=1}^{16}\rho_i(\theta)\rho_j(\theta)\{\left(\widetilde{A}_i + \widetilde{B}_iK_j\right) + \left(E_A\Delta_A(t)F_A + E_B\Delta_B(t)F_BK_j\right)\}x(t) \tag{18}$$

The T-S fuzzy model closed-loop schematic with the PDC controller is shown in Fig. 2.

Lemma 1. ([30]) *Consider some arbitrary X, Y and Z matrices with some compatible dimensions and positive scalar ε, the following LMI is satisfied:*

$$XYZ + Z^TY^TX^T \le \frac{1}{\varepsilon}XX^T + \varepsilon ZZ^T \tag{19}$$

Theorem 1. *The control system (18) is stable in the whole uncertain space if there exists a positive definite matrix X, and positive constants ε_A and ε_B such that the following LMI holds:*

$$G_{ij}=\begin{bmatrix} \Pi & XF_A{}^T & Y_j{}^TF_B{}^T \\ * & -\varepsilon_A I & 0 \\ * & * & -\varepsilon_B I \end{bmatrix}<0 \tag{20}$$

$$\Pi = X\widetilde{A}_i{}^T + \widetilde{A}_iX + Y_j{}^T\widetilde{B}_i{}^T + \widetilde{B}_iY_j + \varepsilon_A E_A E_A{}^T + \varepsilon_B E_B E_B{}^T$$

where i,j are the number of the T-S fuzzy uncertain space, and the number of PDC controller gains.

Proof. Define the candidate Lyapunov function $V = x^TPx$ with positive semi-definite matrix P to derive the stability conditions of the control system. Then, exploiting the T-S fuzzy closed-loop system (18), we have:

$$\dot{V} = \dot{x}^TPx + x^TP\dot{x} < 0 \Rightarrow$$

$$\dot{V} = x^T\sum_{i=1}^{16}\sum_{j=1}^{16}\rho_j(\theta)\rho_i(\theta)\left\{\left(\widetilde{A}_i+\widetilde{B}_iK_j\right)+(E_A\Delta_A(t)F_A+E_B\Delta_B(t)F_BK_j)\right\}^TPx$$

Then, apply Lemma 1 to (23), and the following inequality will be achieved:

$$\sum_{i=1}^{16}\sum_{j=1}^{16}\left(\widetilde{A}_i+\widetilde{B}_iK_j\right)^TP+P\left(\widetilde{A}_i+\widetilde{B}_iK_j\right)+\varepsilon_APE_AE_A{}^TP+\varepsilon_A{}^{-1}F_A{}^TF_A+\varepsilon_BPE_BE_B{}^TP+\varepsilon_B{}^{-1}K_j^TF_B{}^TF_BK_j<0 \tag{24}$$

Using the change of variable trick, and defining $X = P^{-1}$ and $Y_j = K_jP$, we have:

$$X\widetilde{A}_i{}^T+\widetilde{A}_iX+Y_j{}^T\widetilde{B}_i{}^T+\widetilde{B}_iY_j+\varepsilon_BE_BE_B{}^T+\varepsilon_AE_AE_A{}^T+\varepsilon_A{}^{-1}XF_A{}^TF_AX+\varepsilon_B{}^{-1}Y_j^TF_B{}^TF_BY_j\le 0 \tag{25}$$

We can turn (25) into LMI form by using the Schur complement trick twice. Hence, the LMIs formulation will be the same as (20), and the Theorem 1 is proved. ■.

In the following, Lemma 2 is borrowed from [31] where the Tuan relaxation method is used to lower the conservatism of an LMI condition. In this paper, the Tuan relaxation method will be implemented on the final unified LMI condition.

Lemma 2. ([31]) *Suppose we have the stability condition of a T-S fuzzy model with PDC controller as LMI condition G_{ij}. Then, Reducing the conservativeness of G_{ij}, the following sufficient conditions are proposed as:*

$$+x^TP\sum_{i=1}^{16}\sum_{j=1}^{16}\rho_j(\theta)\rho_i(\theta)\left\{\left(\widetilde{A}_i+\widetilde{B}_iK_j\right)+(E_A\Delta_A(t)F_A+E_B\Delta_B(t)F_BK_j)\right\}x<0\Rightarrow$$

$$\dot{V}=x^T\left\{\sum_{i=1}^{16}\sum_{j=1}^{16}\rho_j(\theta)\rho_i(\theta)\left\{\left(\widetilde{A}_i+\widetilde{B}_iK_j\right)+(E_A\Delta_A(t)F_A+E_B\Delta_B(t)F_BK_j)\right\}^TP+P\sum_{i=1}^{16}\sum_{j=1}^{16}\rho_j(\theta)\rho_i(\theta)\left\{\left(\widetilde{A}_i+\widetilde{B}_iK_j\right)+(E_A\Delta_A(t)F_A+E_B\Delta_B(t)F_BK_j)\right\}\right\}x<0 \tag{21}$$

Obviously, (21) holds if the following inequality holds:

$$\sum_{i=1}^{16}\sum_{j=1}^{16}\rho_j(\theta)\rho_i(\theta)\left\{\left(\widetilde{A}_i+\widetilde{B}_iK_j\right)+(E_A\Delta_A(t)F_A+E_B\Delta_B(t)F_BK_j)\right\}^TP$$

$$+P\sum_{i=1}^{16}\sum_{j=1}^{16}\rho_j(\theta)\rho_i(\theta)\left\{\left(\widetilde{A}_i+\widetilde{B}_iK_j\right)+(E_A\Delta_A(t)F_A+E_B\Delta_B(t)F_BK_j)\right\}<0 \tag{22}$$

One knows that $\rho_i(\theta)>0$ and $\rho_j(\theta)>0$ for (i = 1,…,16) and (j = 1,..,16). Therefore, we have:

$$\left\{\sum_{i=1}^{16}\sum_{j=1}^{16}\left\{\left(\widetilde{A}_i+\widetilde{B}_iK_j\right)+(E_A\Delta_A(t)F_A+E_B\Delta_B(t)F_BK_j)\right\}^TP+P\sum_{i=1}^{16}\times\sum_{j=1}^{16}\left(\left\{\widetilde{A}_i+\widetilde{B}_iK_j)+(E_A\Delta_A(t)F_A+E_B\Delta_B(t)F_BK_j)\right\}\right\}<0\Rightarrow$$

$$\sum_{i=1}^{16}\sum_{j=1}^{16}\left(\widetilde{A}_i+\widetilde{B}_iK_j\right)^TP+P\left(\widetilde{A}_i+\widetilde{B}_iK_j\right)+(E_A\Delta_A(t)F_A)^TP+P(E_A\Delta_A(t)F_A)+(E_B\Delta_B(t)F_BK_j)^TP+P\left(E_B\Delta_B(t)F_BK_j\right)<0 \tag{23}$$

$$\begin{cases} G_{ii}<0; i=1,\cdots,r=2^r \\ \dfrac{1}{r-1}G_{ii}+\dfrac{1}{2}(G_{ij}+G_{ji})<0; i,j=1,\cdots,r=2^r; i\ne j \end{cases} \tag{26}$$

3.3. Optimal T-S fuzzy controller design

Theorem 2. *The following LQR cost function in (27a) will be optimized for the T-S fuzzy model (18) if the LMI in (27b) holds.*

$$\min\int_0^{250}x^TQ_fx+u^TR_fu \tag{27a}$$

$$S.t\begin{bmatrix} \psi & XF_A{}^T & Y_j{}^TF_B{}^T & Y_j{}^T & X \\ * & -\varepsilon_AI & 0 & 0 & 0 \\ * & * & -\varepsilon_BI & 0 & 0 \\ * & * & * & -R_f{}^{-1} & 0 \\ * & * & * & * & -Q_f{}^{-1} \end{bmatrix}<0 \tag{27b}$$

where

$\psi = X\widetilde{A}_i{}^T+\widetilde{A}_iX+Y_j{}^T\widetilde{B}_i{}^T+\widetilde{B}_iY_j+\varepsilon_AE_AE_A{}^T+\varepsilon_BE_BE_B{}^T, (i=1,..,16; j=1,\cdots,16)$ X, Q_f and R_f are positive-semi-

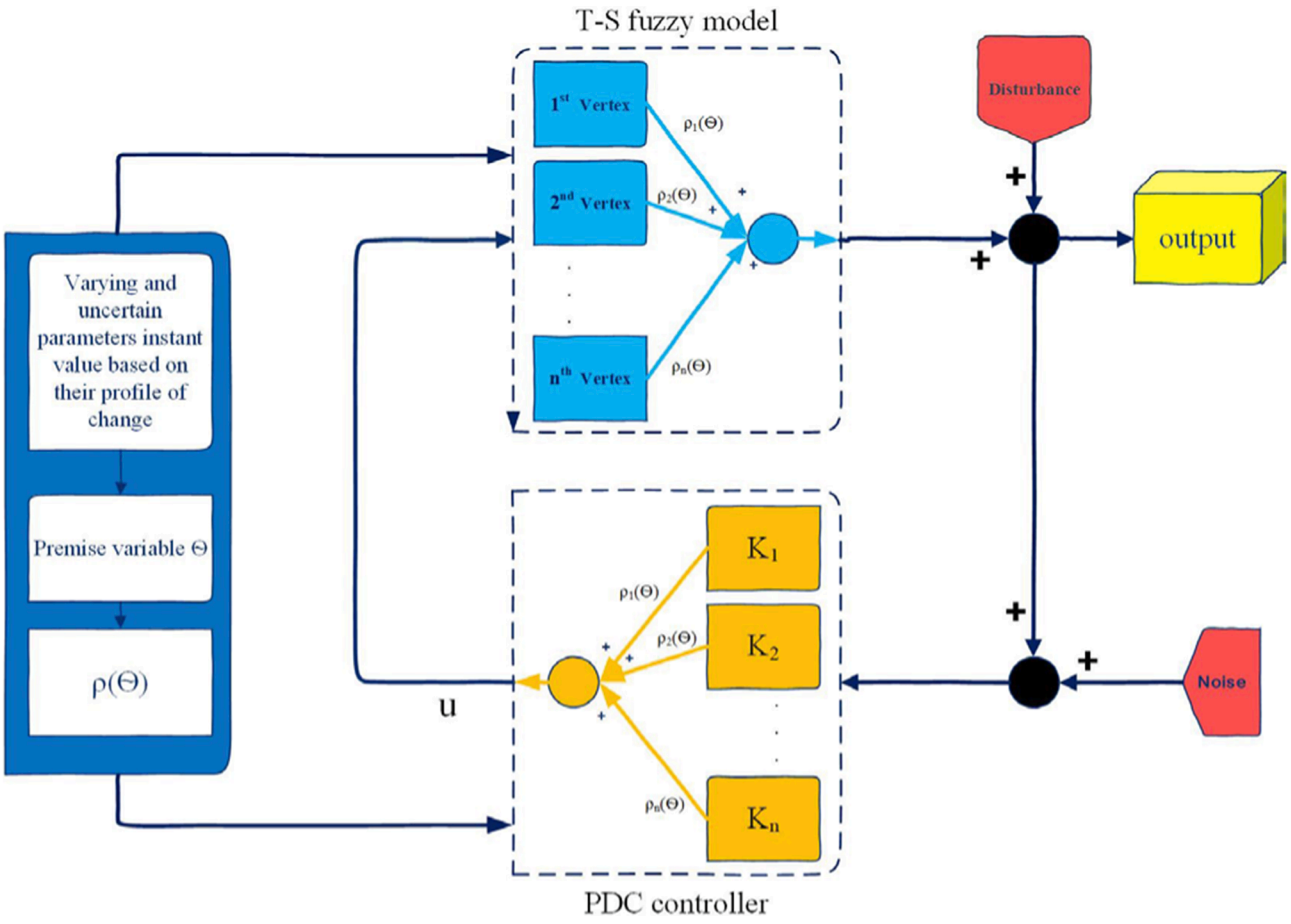

Fig. 2. T-S fuzzy model and PDC controller design process for closed-loop interconnection added by disturbance and noise graph as an online process.

definite matrices.

Proof. The LMI condition of LQR minimization can be concluded from [25] as:

$$\begin{bmatrix} X\widetilde{A}_i^{\,T} + \widetilde{A}_i X + Y_j^{\,T}\widetilde{B}_i^{\,T} + \widetilde{B}_i Y_j & Y_j^{\,T} & X^T \\ Y_j & -R_f^{\,-1} & 0 \\ X & 0 & -Q_f^{\,-1} \end{bmatrix} < 0 \tag{28}$$

Now, LMIs (20) and (28) can be rewritten in a compact form to assure stability and optimized LQR cost function, simultaneously. The $(1,1)$ entry of (28) is the general condition of a system stabilization. Therefore, extending the T-S fuzzy system stabilization condition to the mentioned LQR optimization (28), the $(1,1)$ entry of (28) will be replaced with LMI in (20). Using the wide form of (28) for the mixed LMI condition of stabilizing the T-S fuzzy system added to the LQR optimization, we have:

$$\begin{bmatrix} \psi & XF_A^{\,T} & Y_j^{\,T}F_B^{\,T} \\ * & -\varepsilon_A I & 0 \\ * & * & -\varepsilon_B I \end{bmatrix} + Y_j^{\,T}R_f^{\,-1}Y_j + X^T Q_f^{\,-1} X < 0 \tag{29}$$

Using the Schur complement lemma, the completed version of the LMI (27b) is concluded. ■.

Remark 1. *The controller gain calculated by employing Theorem 1 is entirely applicable and reasonable in terms of mathematical calculations. However, the result might not be that suitable for the existing system. Therefore, we utilized Theorem 2 to make the simulations more compatible with the existing system. Optimizing (29) will result in desired value of the control input signals (prioritizing the control signals).*

3.4. Robust T-S fuzzy controller design

The system of covid-19 spread is usually full of disturbances. For instance, there are some kinds of gatherings and ceremonies that make a part of the population sick. Also, noise affects the model because the number of infected individuals is not exact due to lack of enough testing. Therefore, designing a controller which copes with such problems seems necessary. This is the reason why Theorem 3 is utilized in the following.

Assume (18) is affected by noise and disturbance inputs. Considering a single performance channel y and the two external inputs as the noise and the disturbance, the T-S fuzzy system will be formed as (30).

$$\dot{x} = \left[\sum_{i=1}^{16} \sum_{j=1}^{16} \rho_j(\theta)\rho_i(\theta)\{(\widetilde{A}_i + \widetilde{B}_i K_j)\}x(t) \right] + B_w w + B_n n \tag{30}$$

where $B_w = [0;1;0;0]$ and $B_n = [0;1;0;0]$.

The following theorem aims to establish robust stability and at the same time, disturbance and noise attenuation. Please note that disturbance w is assumed to be bounded in this paper, where $\|w(t)\|_2 \leq \widehat{w}$.

Theorem 3. *The problem of the mixed $H_2 - H_\infty$ norm minimization for a performance channel y could be optimized for the T-S fuzzy model stability*

added to LQR optimization in (27b), if one can acquire a feasible solution for the following LMI-based optimization problem:

$$\min_{X_1,X_2,\gamma_1,\gamma_2} \gamma_1+\gamma_2 \tag{31a}$$

S.t.

$$\begin{bmatrix} \psi & XF_A{}^T & Y_j{}^TF_B{}^T & X & Y_j{}^T & B_w & X_1C^T & X_2B_n \\ * & -\varepsilon_A I & 0 & 0 & 0 & 0 & 0 & 0 \\ * & * & -\varepsilon_B I & 0 & 0 & 0 & 0 & 0 \\ * & * & * & -Q_f{}^{-1} & 0 & 0 & 0 & 0 \\ * & * & * & * & -R_f{}^{-1} & 0 & 0 & 0 \\ * & * & * & * & * & -\gamma_1{}^2 I & 0 & 0 \\ * & * & * & * & * & * & -I & 0 \\ * & * & * & * & * & * & * & -I \end{bmatrix} <0 \tag{31b}$$

$$\begin{bmatrix} X_2 & X_2C^T \\ CX_2 & \gamma_2{}^2 I \end{bmatrix} >0 \tag{31c}$$

$$\psi = X\widetilde{A}_i{}^T + \widetilde{A}_iX + Y_j{}^T\widetilde{B}_i{}^T + \widetilde{B}_iY_j + \varepsilon_A E_A E_A{}^T + \varepsilon_B E_B E_B{}^T$$

Proof. The LMI conditions of H_2-H_∞ norm minimization for linear systems has been previously proved [32–38] and presented as:

$$\min_{X_1,X_2,\gamma_1,\gamma_2} \gamma_1+\gamma_2 \tag{32a}$$

S.t.

$$\begin{bmatrix} X_1\widetilde{A}_i{}^T + \widetilde{A}_iX_1 + Y_j{}^T\widetilde{B}_i{}^T + \widetilde{B}_iY_j & B_w & X_1C^T \\ B_w{}^T & -\gamma_1{}^2 I & 0 \\ CX_1{}^T & 0 & -I \end{bmatrix} <0 \tag{32b}$$

$$\begin{bmatrix} X_2\widetilde{A}_i{}^T + \widetilde{A}_iX_2 + Y_j{}^T\widetilde{B}_i{}^T + \widetilde{B}_iY_j & X_2B_n \\ B_n{}^TX_2 & -I \end{bmatrix} <0 \tag{32c}$$

$$\begin{bmatrix} X_2 & X_2C^T \\ CX_2 & \gamma_2{}^2 I \end{bmatrix} >0 \tag{32d}$$

If the above LMIs are satisfied, the mixed H_2-H_∞ norm minimization is guaranteed. Here, the extension of these LMIs to TS fuzzy models is done where the (32b) and (32c) LMIs will be mixed with the one we already have in (27b). Extending theorem 3 to the T-S fuzzy model, as we mentioned in the proof of theorem 2, in the (32b) and (32c) LMIs the $(1,1)$ entry will be replaced with the LMI in (27b). Similar as the proof of theorem 2, and using the wide form of (32b) and (32c) mixed together, one has:

$$\Gamma+\gamma_1{}^2B_w^TB_w + X_1C^TCX_1 + X_2B_nB_n{}^TX_2 < 0 \tag{33}$$

where Γ is the LMI in (27b).

The final unified LMI condition (31b) for the proposed multi-objective controller can be achieved utilizing the Schur complement to (32). Consequently, the overall multi-objective problem is to solve (31a) minimization subject to (32b) and (32c) LMIs which conclude both stability and performance. ■.

Remark 2. *It should be noted that what we called H_∞ norm and H_2 norm in this work, could be equivalently be seen as "induced L_2-L_2 norm" and "generalized H_2 norm" or "L_2-L_∞ norm" terms in the literature [32–39].*

Remark 3. *We will consider $X_1=X_2=X$ and solve the problem with this assumption. The assumption will help us to lower the conservatism of the solution. Tuan relaxation will also be applied to Theorem 2 and Theorem 3 as well as Theorem 1 to relax the conservativeness of each LMIs.*

4. Simulation results

In this section, the simulation results are proposed. The results are shown in the following three scenarios:

- First scenario: Open-loop and closed-loop response differences
- Second scenario: The designed controller comparison with some conventional controllers
- Third scenario: Effects of time-delayed vaccination as control input

The time frame for the simulation to be deployed is 300 days for all the scenarios. The initial conditions of the states, the model parameters values, and the other needed matrices are defined in Table 1. The disturbance input applied to the model is also plotted in Fig. 3.

4.1. First scenario: Open loop and closed-loop response differences

In the first scenario, the open and the closed-loop (with controller) response results are presented and compared to see how different the results would be if there were no control action for the coronavirus spread. Fig. 4 shows that with applying the control measures, the number of infected cases decrease and the recovered cases increase. The other important point which can be concluded from Fig. 4 is that the control measures can damp the peak in the number of infected persons to some good points. So, as peaking at the number of infected cases is disastrous for countries, it will be very crucial for them to take counteractive actions at the right time. The control inputs for the closed-loop response can be seen in Fig. 5. Another important factor is that a coefficient of infected cases can be interpreted as number of deceased persons. Therefore, based on Fig. 6 we can find out that utilizing the control inputs will end up with a great decrement in the number of deceased cases.

In another study, we decided to show the approach's performance when a model change happens. Therefore, in this part, we considered the primary SIRQ covid-19 model in [24] without any modification as the reference model. We also simulated the model with a different initial condition from the initial values of Table 1 in Fig. 7 and Fig. 8. The results of our proposed method on the model with and without modification (our model in (1) and the model in [24]) are almost similar, and the reason is that the proposed method does not depend on the model parameters, initialization or structure.

Based on Theorem 2, we regulated the control inputs to some desired

Table 1
List of the unknown parameters and initial conditions of the covid-19 model.

Parameter (or matrices)	Definition	Value
S_0	Susceptible compartment's initial value	1,000,000 (persons)
I_0	Infected compartment's initial value	100 (persons)
R_0	Recovered compartment's initial value	100 (persons)
Q_0	Deceased compartment's initial value	500 (persons)
β	Transmission rate	0.307 (person per days)
γ	Removal rate (from infected compartment)	0.030 (person per days)
δ	Quarantine rate	0.073 (person per days)
ζ	Reinfection rate	0.00726 (person per day)
κ	Removal rate (from quarantined compartment)	0.0033 (person per day)
$\hat{w}$	2norm of disturbance	10,000
C	–	[0100]
D	–	[000]
R_f	–	$diag(80, 9000, 1)$
Q_f	–	I_4

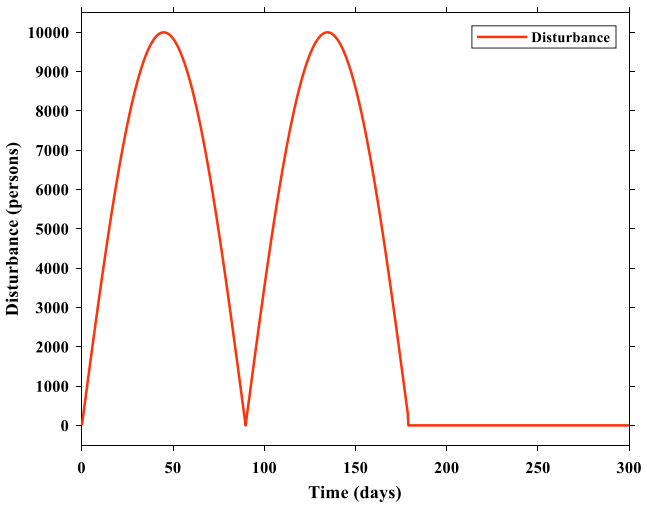

Fig. 3. The suggested bounded disturbance input on the system.

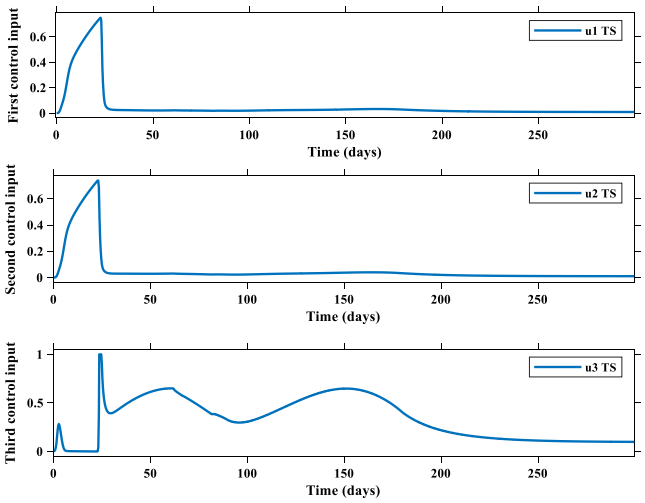

Fig. 5. Control inputs u_1 (social distancing and lockdown), u_2 (treatments), and u_3 (vaccination) for closed-loop PDC controller response as controlling interventions to deal with the corona-virus spread.

values because the cost of applying high degrees of social distancing and medical treatment on societies is extortionate for the authorities. We also translate the control input u_1 as a suggested strategy presented in Table 2 to clarify the results for reader's better understanding. The control inputs u_2, u_3 can also be translated as the treatment rate and the vaccination rate for the people of society.

4.2. *Second scenario: The designed controller comparison with some conventional controllers*

In this scenario, different control approaches are considered to see how they affect the system's closed-loop response. The approaches for the comparison are the proposed T-S fuzzy controller, robust LPV

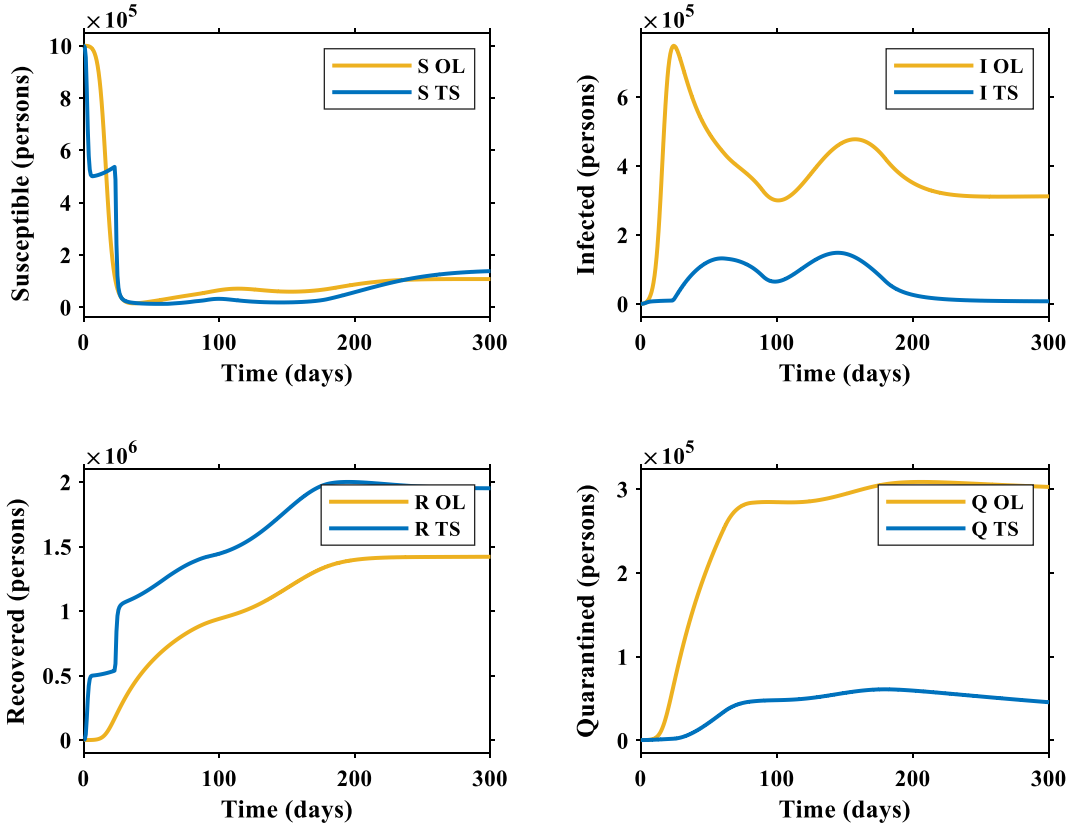

Fig. 4. States of the covid-19 model for the closed-loop with PDC controller (blue) and the open-loop response (yellow) where the effects of implementing a suitable control strategy could be seen obviously. (For interpretation of the references to colour in this figure legend, the reader is referred to the web version of this article.)

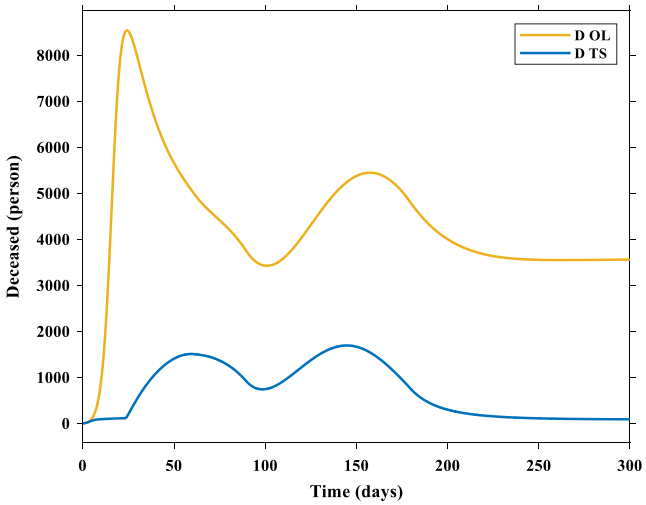

Fig. 6. The number of deceased persons when with control interventions (blue) and without control interventions (yellow). (For interpretation of the references to colour in this figure legend, the reader is referred to the web version of this article.)

controller, and state feedback (SF) LPV controller, which can be interpreted as a robust controller. From now on, and for simplicity, we will mention the robust LPV and state feedback LPV approaches with LPV and SF abbreviations, respectively. It should be noted that the robust LPV approach for this part is borrowed from our previous work [25], which is mixed with two other works [40,41] to improve the desired response. Fig. 9 and Fig. 10 show lower amounts of control inputs for the SF approach than the other two approaches, and it is because there are no LQR constraints in this approach to regulate the control values. There will be even more infected individuals, and fewer recovered people for the SF approach than the other two approaches. These explanations underline the importance of using LQR in this problem.

We can observe a slight difference in LPV and T-S method responses with fewer infected and quarantined cases for the T-S fuzzy method than for the LPV method. Also, based on the explanations in section 3, we already knew that considering the mathematical computations, the T-S fuzzy method that we proposed in this paper could be a better choice than the LPV method. A suggested parameter's variation for β, δ are also

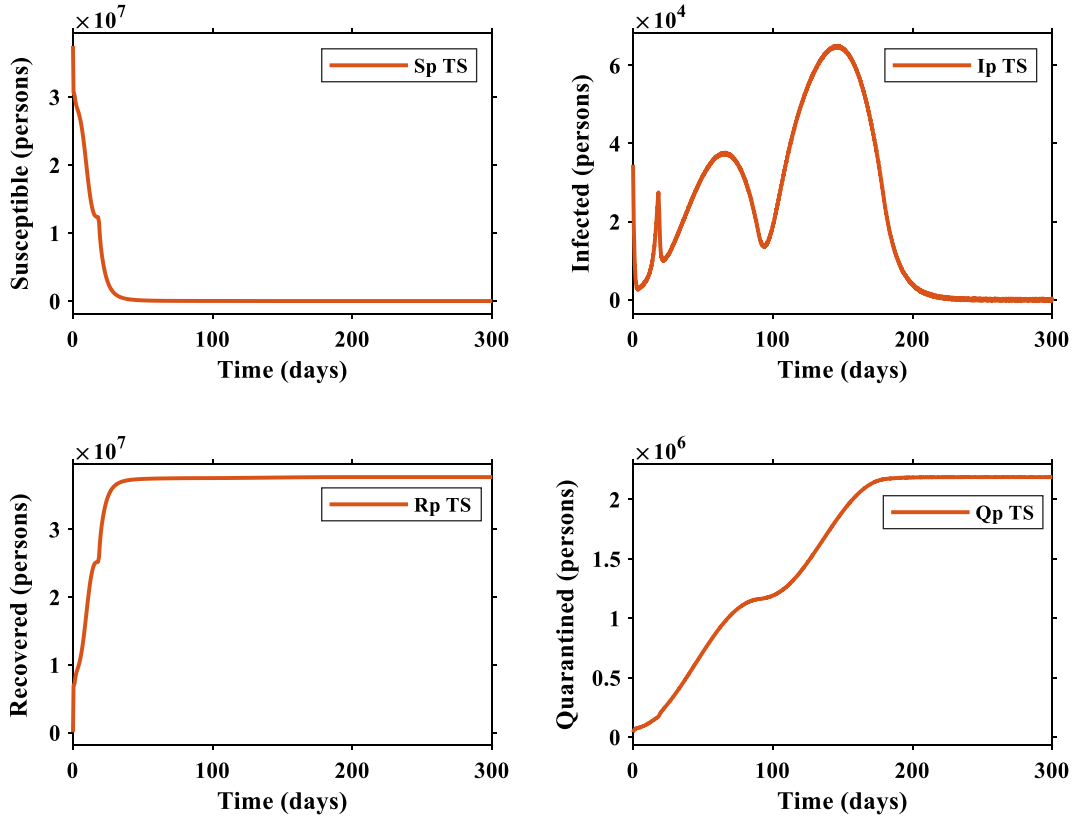

Fig. 7. The state of the covid-19 model in [24].

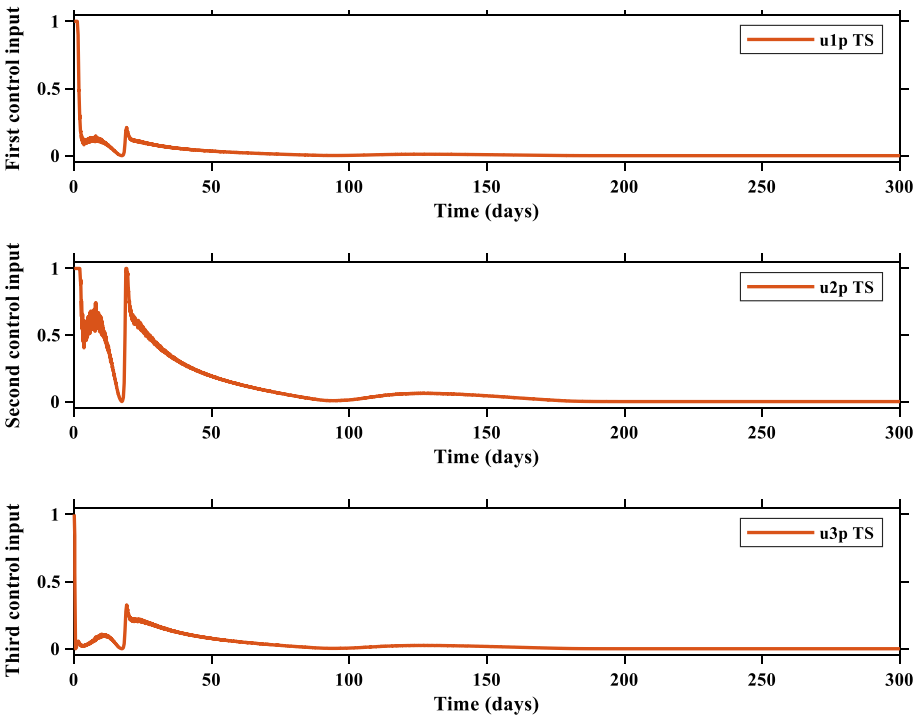

Fig. 8. The control inputs of the covid-19 model in [24].

Table 2
The social distancing suggested policy as a practical example.

Control input u_1 (social distancing)	Action
$0 \leq u_1 \leq 0.3$	Regular activity for all sectors and sections of the society and wearing face masks
$0.3 \leq u_1 \leq 0.5$	Obligatory use of face masks in public and restrictive activities in less important offices and bureaus
$0.5 \leq u_1 \leq 0.7$	Restriction in every part of society and economy to some extent
$0.7 \leq u_1 \leq 1$	Rigid restriction in all parts

depicted in Fig. 11 where they decrease within the considered duration. Determining the variation profile of these parameters more precisely will conclude more realistic results. It can also be noted that the parameters' profile of variation will not affect the stability of the system. The effective reproduction number is also plotted in Fig. 12. It shows that all the mentioned methods can adequately lower the contagiousness of the coronavirus and lead the effective reproduction number to a final value of less than one, which is equivalent to controlling covid-9 spread. It will cause a further burden on authorities to intensify the restrictions lowering higher amounts of effective reproduction number.

The H_2 and H_∞ norms of the system in each method are also pointed out in Table 3. The number of deceased persons with different approaches is shown in Fig. 13 revealing that the T-S fuzzy method has the lowest number of deceased cases.

4.3. Third scenario: Effects of time-delayed vaccination as control input

Dealing with coronavirus spread worldwide has been a hot topic for recent two years. Some countries pioneered in applying the control measures, especially vaccination. Based on what we have seen in the coronavirus statistics in all countries, it can be concluded that vaccinating society as fast as possible is very crucial and effective in coping with casualties of the coronavirus. In doing so, we compared two situations implementing vaccination with and without delays to the T-S fuzzy model. This part considers 100 days of delay, and the results are presented in Fig. 14. It can be seen that the delay makes trouble in states convergence, and it makes the states' trajectories very sensitive to control inputs than the situation in which there is no delay for the third control input. Based on Fig. 14, the convergence of the fourth state which is quarantined compartment is a bit slower than the other states and need more time than the simulation time to fully converge.

Moreover, one of the other adverse effects of the delay can be seen from Fig. 15 where higher amounts of control input are needed in the delayed situation. We conclude that the delay makes the states and the control input oscillate around their final values. According to Fig. 16, the effective reproduction number for delayed cases has a slower convergence. In addition, the covid-19 spread in not fully controlled in delayed case because the effective reproduction value is not settled on a value lower than one. Thus, this simulation's scenario showed how dangerous the situation could get if the vaccination as a controlling intervention did not apply within a suitable time.

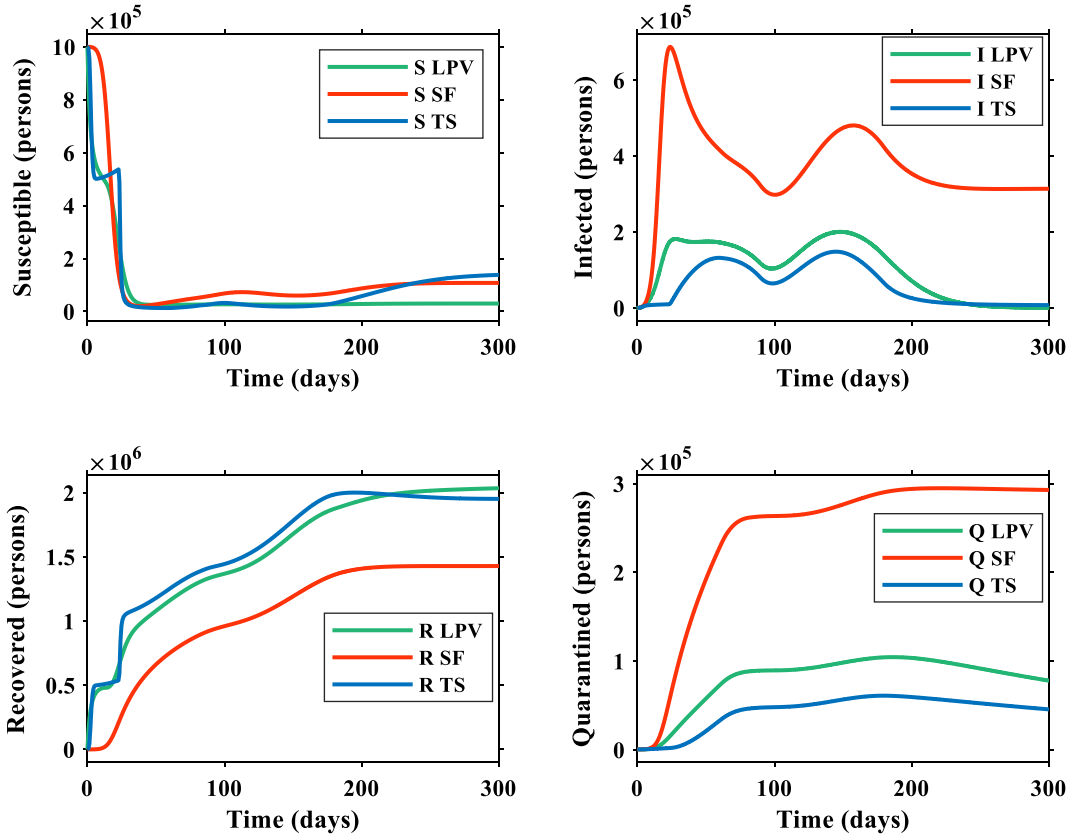

Fig. 9. States of the covid-19 model for comparing LPV (green), simple state feedback (red), and T-S fuzzy (blue) approaches with the T-S fuzzy and LPV approaches outperforming the state feedback controller. (For interpretation of the references to colour in this figure legend, the reader is referred to the web version of this article.)

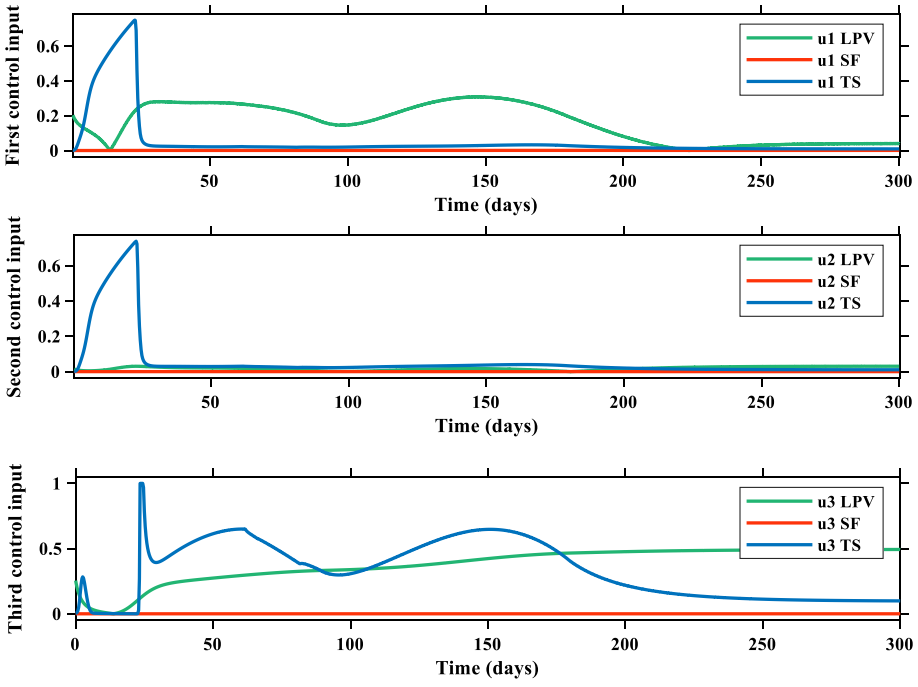

Fig. 10. The control inputs for comparing LPV (green), simple state feedback (red), and T-S fuzzy (blue) approaches with the T-S fuzzy approach having the most optimum control effort. (For interpretation of the references to colour in this figure legend, the reader is referred to the web version of this article.)

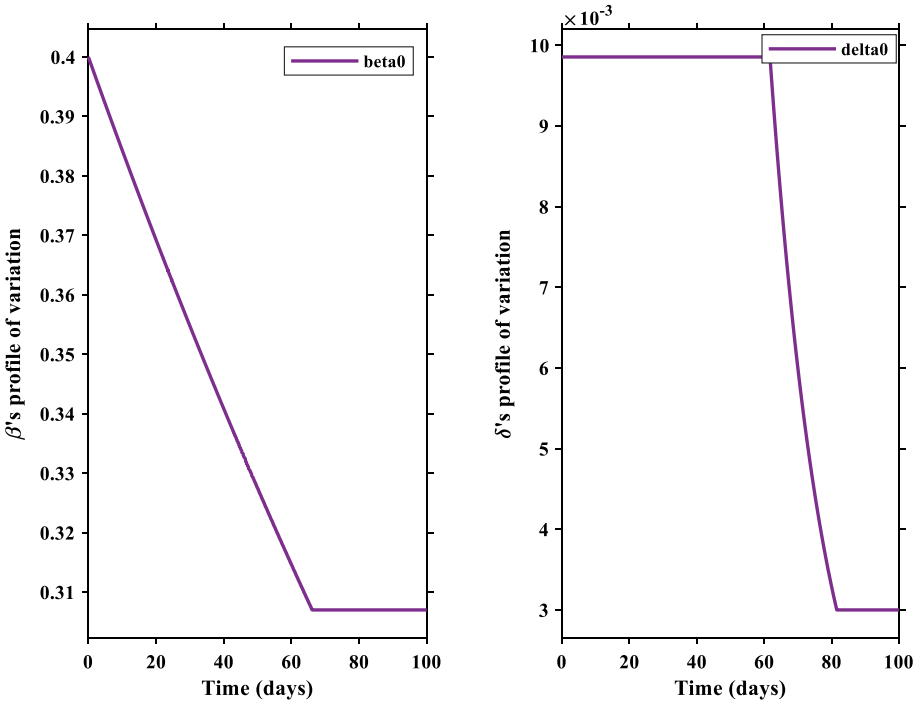

Fig. 11. Suggested profiles of variations for β and..δ

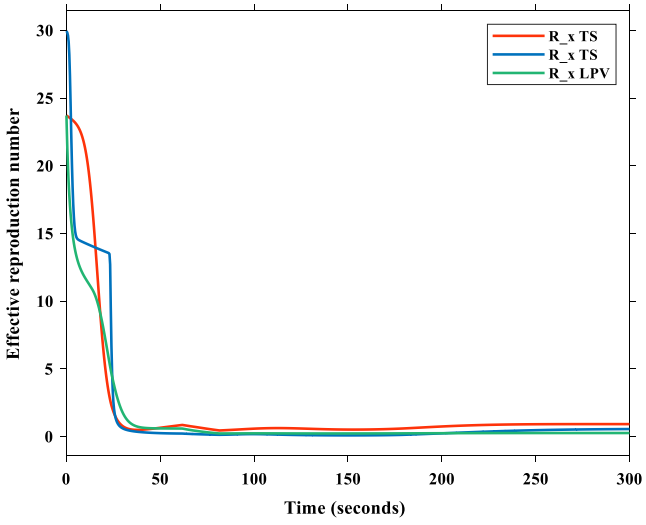

Fig. 12. Effective reproduction number during the simulation time for different control approaches with T-S fuzzy as lead controller.

Table 3
The H_2 and H_∞ norms of the system in each method.

	H_2 norm	H_∞ norm
T-S fuzzy method	0.9956	2.0353
Robust LPV method	1.7373	5.0827
State feedback method	$\approx$ 0.0076	$\approx$ 115.7413

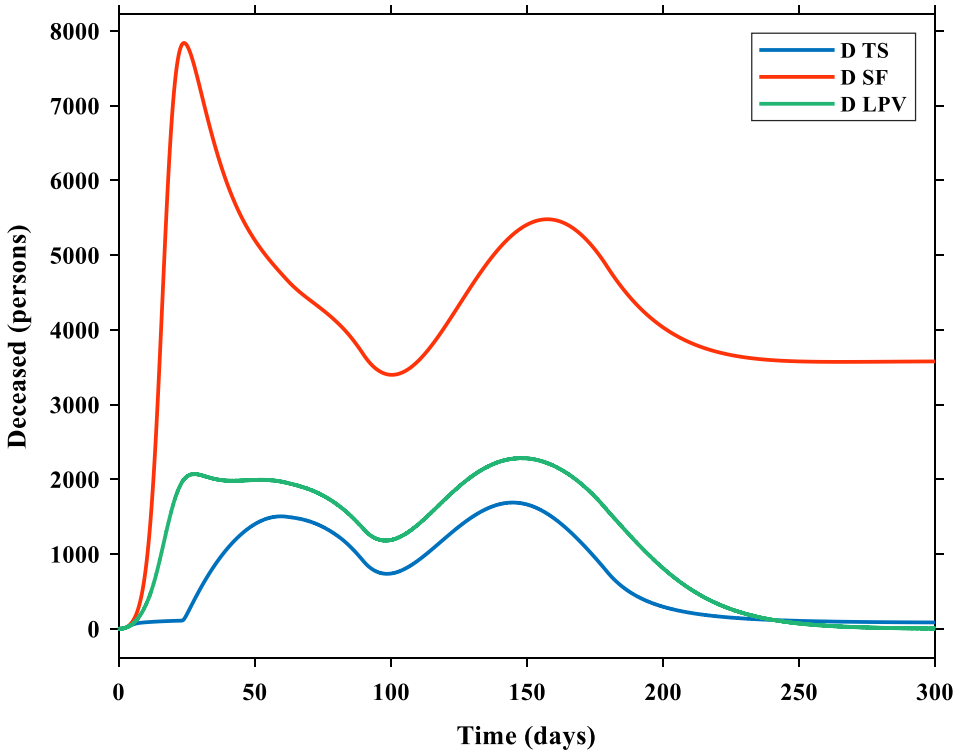

Fig. 13. The number of deceased persons for different approaches: T—S fuzzy (blue), robust LPV (green), and state feedback (red). (For interpretation of the references to colour in this figure legend, the reader is referred to the web version of this article.)

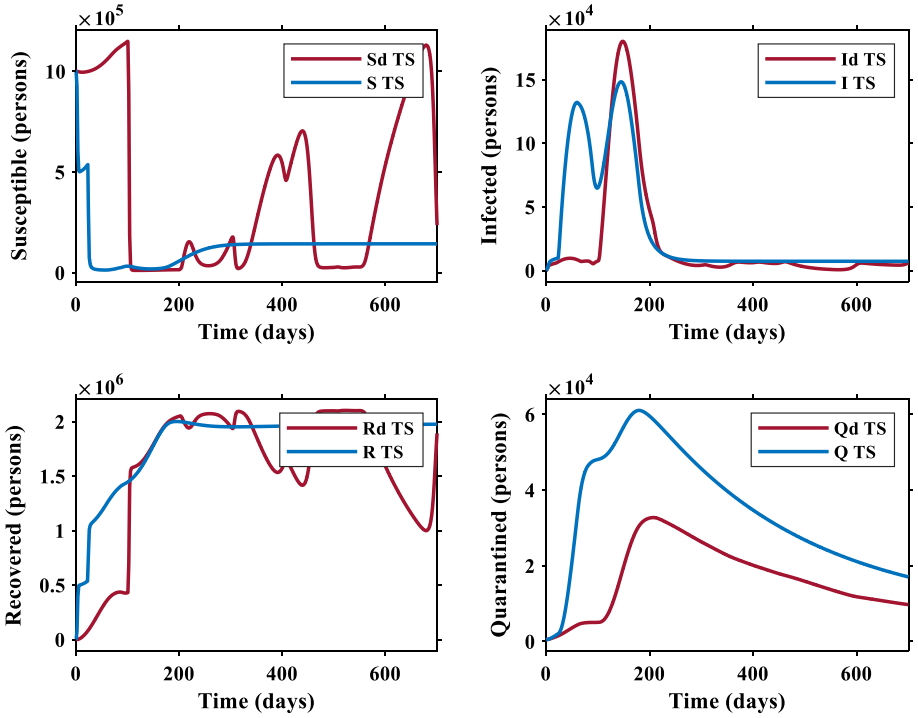

Fig. 14. The states of coronavirus model with 100 days of delay (dark red) and without implementing delay (blue) to the third control inputs showing the disastrous consequences of the delay. (For interpretation of the references to colour in this figure legend, the reader is referred to the web version of this article.)

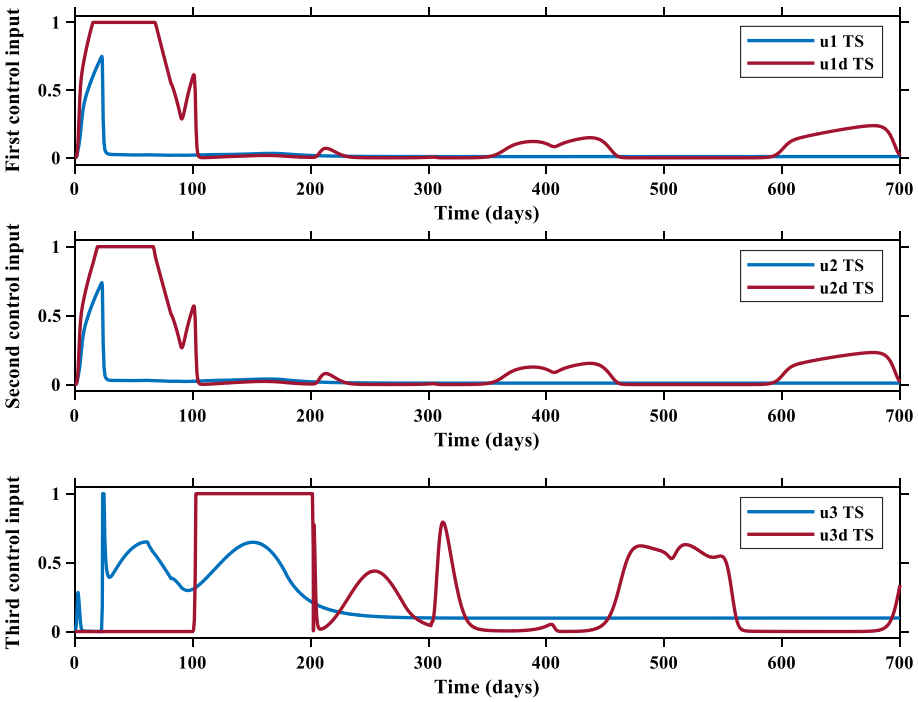

Fig. 15. The control inputs with and without implementing 100 days of delay to the third control inputs.

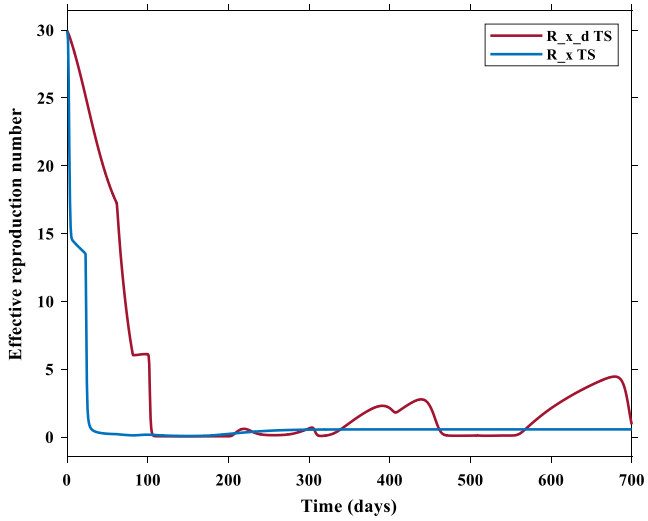

Fig. 16. Effective reproduction number during the simulation time with and without delay stressing the importance of vaccination in controlling the pandemic.

5. Conclusion and future work

In this article, T-S fuzzy modeling of coronavirus spread is exploited considering uncertain and varying parameters. Then, a feedback controller law is used to simultaneously solve a multi-objective control problem, including model stabilization, mixed $H_2 - H_\infty$ norm minimization, and optimal LQR problem. Note that the T-S fuzzy approach presented in this paper, can be beneficial dealing with large-scale systems, systems with lots of uncertainties, varying parameters, and nonlinearities. Next, the results of controller design are simulated and analyzed comparatively in three parts. As a result, it can be concluded that dealing with the coronavirus highlights the effects of using suitable strategies for controlling interventions. Also, a suggested policy for control actions is presented, which can be used in different countries accordingly. For future work, we can consider some data-based methods or other online model-based control methods like MPC to compare the results and the efficiency of different approaches for this specific application. Also, another research direction is to provide a model from a real dataset, design the appropriate controller with the proposed approach and study the effects of the controller on the whole population dataset.

CRediT authorship contribution statement

Reza Najarzadeh: Conceptualization, Methodology, Software, Writing – original draft. **Mohammad Hassan Asemani:** Conceptualization, Software, Supervision, Writing – review & editing. **Maryam Dehghani:** Conceptualization, Software, Supervision, Writing – review & editing. **Mokhtar Shasadeghi:** Investigation, Writing – review & editing.

Declaration of Competing Interest

The authors declare that they have no known competing financial interests or personal relationships that could have appeared to influence the work reported in this paper.

References

[1] H. Verma, V.N. Mishra, P.J.I.T. Mathur, Effectiveness of lock down to curtail the spread of corona virus: a mathematical model, ISA Trans. (2021).
[2] J. Riou, C.L. Althaus, Pattern of early human-to-human transmission of Wuhan 2019 novel coronavirus (2019-nCoV), December 2019 to January 2020, Eurosurveillance 25 (4) (2020) 1–5.
[3] C. Treesatayapun, Epidemic model dynamics and fuzzy neural-network optimal control with impulsive traveling and migrating: case study of COVID-19 vaccination, Biomed. Signal Process. Control 71 (2022) 103227.
[4] J.S. Tregoning, K.E. Flight, S.L. Higham, Z. Wang, B.F. Pierce, Progress of the COVID-19 vaccine effort: viruses, vaccines and variants versus efficacy, effectiveness and escape, Nat. Rev. Immunol. 21 (10) (2021) 626–636.
[5] L. Corey, J.R. Mascola, A.S. Fauci, F.S. Collins, A strategic approach to COVID-19 vaccine R&D, Science 368 (6494) (2020) 948–950.
[6] C. Aschwanden, Five reasons why COVID herd immunity is probably impossible, Nature (2021) 520–522.
[7] C. Huang, et al., Clinical features of patients infected with 2019 novel coronavirus in Wuhan, China, Lancet 395 (10223) (2020) 497–506.

[8] WHO, Worldometers: Coronavirus cases, 2022, Available from: <https://www.worldometers.info/coronavirus/>.
[9] S. Shen, How much coronavirus testing is enough? States could learn from retailers as they ramp up, 2020, Available from <https://theconversation.com/how-much-coronavirus-testing-is-enough-states-could-learn-from-retailers-as-they-ramp-up-136494>.
[10] P. Van den Driessche, J. Watmough, Further notes on the basic reproduction number, in: Mathematical Epidemiology, Springer, 2008, pp. 159–178.
[11] S. Lu, Z. Zhu, J.M. Gorriz, S.H. Wang, Y.D.J. Zhang, NAGNN: classification of COVID-19 based on neighboring aware representation from deep graph neural network, Int. J. Intell. Syst. 37 (2) (2022) 1572–1598.
[12] S. Lu, S.-H. Wang, Y.-D. Zhang, Detection of abnormal brain in MRI via improved AlexNet and ELM optimized by chaotic bat algorithm, Neural Comput. Appl. 33 (17) (2021) 10799–10811.
[13] I. Cooper, A. Mondal, C.G. Antonopoulos, A SIR model assumption for the spread of COVID-19 in different communities, Chaos Solitons Fractals 139 (2020), 110057.
[14] J. Satsuma, R. Willox, A. Ramani, B. Grammaticos, A. Carstea, Extending the SIR epidemic model, Phys. A: Stat. Mech. Appl. 336 (3–4) (2004) 369–375.
[15] Z. Memon, S. Qureshi, B.R. Memon, Assessing the role of quarantine and isolation as control strategies for COVID-19 outbreak: a case study, Chaos Solitons Fractals 144 (2021), 110655.
[16] M.M. Morato, I.M. Pataro, M.V.A. da Costa, J.E. Normey-Rico, A parametrized nonlinear predictive control strategy for relaxing COVID-19 social distancing measures in Brazil, ISA Trans. (2020).
[17] A. Rajaei, M. Raeiszadeh, V. Azimi, M. Sharifi, State estimation-based control of COVID-19 epidemic before and after vaccine development, J. Process Control 102 (2021) 1–14.
[18] W. Wei, B. Duan, M. Zuo, Q. Zhu, An extended state observer based U-model control of the COVID-19, ISA Trans. (2021).
[19] N. Talkhi, N.A. Fatemi, Z. Ataei, M.J. Nooghabi, Modeling and forecasting number of confirmed and death caused COVID-19 in IRAN: a comparison of time series forecasting methods, Biomed. Signal Process. Control 66 (2021), 102494.
[20] M.A. Hadi, H.I. Ali, Control of COVID-19 system using a novel nonlinear robust control algorithm, Biomed. Signal Process. Control 64 (2021), 102317.
[21] R. Abolpour, S. Siamak, M. Mohammadi, P. Moradi, M. Dehghani, Linear parameter varying model of COVID-19 pandemic exploiting basis functions, Biomed. Signal Process. Control 70 (2021), 102999.
[22] A. Hasan, Y. Nasution, A compartmental epidemic model incorporating probable cases to model COVID-19 outbreak in regions with limited testing capacity, ISA Trans. (2021).
[23] H. Verma, V.N. Mishra, P. Mathur, Effectiveness of lock down to curtail the spread of corona virus: a mathematical model, ISA Trans. (2021).
[24] W. Zheng, Total variation regularization for compartmental epidemic models with time-varying dynamics, arXiv preprint arXiv:.00412, 2020.
[25] R. Najarzadeh, M. Dehghani, M.H. Asemani, R. Abolpour, Optimal robust LPV control design for novel Covid-19 disease, J. Control, Special issue 14 (5) (2021) 141–153.
[26] G. Massonis, J.R. Banga, A.F.J. Aric Villaverde, Structural identifiability and observability of compartmental models of the COVID-19 pandemic, Ann. Rev. Control 51 (2021) 441–459.
[27] P. Van den Driessche, J. Watmough, Reproduction numbers and sub-threshold endemic equilibria for compartmental models of disease transmission, Math. Biosci. 180 (1–2) (2002) 29–48.
[28] M.H. Asemani, V.J. Majd, A robust $ H_ {\infty} $ non-PDC design scheme for singularly perturbed T-S fuzzy systems with immeasurable state variables, IEEE Trans. Fuzzy Syst. 23 (3) (2014) 525–541.
[29] M. Farbood, Z. Echreshavi, M. Shasadeghi, Parameter varying model predictive control based on T-S fuzzy model using QP approach: a case study, Iran. J. Sci. Technol. Trans. Electr. Eng. 43 (1) (2019) 269–276.
[30] K. Zare, M. Shasadeghi, A. Izadian, T. Niknam, M.H. Asemani, Switching TS fuzzy model-based dynamic sliding mode observer design for non-differentiable nonlinear systems, Eng. Appl. Artif. Intell. 96 (2020), 103990.
[31] H.D. Tuan, P. Apkarian, T. Narikiyo, Y. Yamamoto, Parameterized linear matrix inequality techniques in fuzzy control system design, IEEE Trans. Fuzzy Syst. 9 (2) (2001) 324–332.
[32] C. Scherer, S. Weiland, Linear matrix inequalities in control, in: Lecture Notes, Dutch Institute for Systems Control, Delft, The Netherlands, vol. 3, no. 2, 2000.
[33] A. Fakharian, V. Azimi, Robust mixed-sensitivity H∞ control for a class of MIMO uncertain nonlinear IPM synchronous motor via TS fuzzy model, in: 2012 17th International Conference on Methods & Models in Automation & Robotics (MMAR), IEEE, 2012, pp. 546–551.
[34] D. Allahverdy, A. Fakharian, Robust H_2 / H_∞ multi objective controller design with Takagi-Sugeno fuzzy model for a mobile two-wheeled inverted pendulum, Int. J. Smart Electr. Eng. 11 (01) (2022) 13–20.
[35] V. Azimi, M.B. Menhaj, A. Fakharian, Tool position tracking control of a nonlinear uncertain flexible robot manipulator by using robust H2/H∞ controller via T-S fuzzy model, Sadhana 40 (2) (2015) 307–333.
[36] Y. Peng, Q. Zhu, H. Nouri, Mixed H2/H∞ robust controller design based LMI techniques, in: Applied Methods Techniques for Mechatronic Systems: Modelling, Identification Control, vol. 452, 2013, p. 325.
[37] M.A. Rotea, The generalized H2 control problem, Automatica 29(2) (1993) 373–385.
[38] P. Ma, Z. Zhu, L. Sheng, Static output feedback H 2/H∞ control with spectrum constraints for stochastic systems subject to multiplicative noises, Syst. Sci. Control Eng. 6 (3) (2018) 118–125.
[39] K. Zhou, J.C. Doyle, Essentials of Robust Control, Prentice Hall, Upper Saddle River, NJ, 1998.
[40] C. Olalla, R. Leyva, A. El Aroudi, I. Queinnec, Robust LQR control for PWM converters: an LMI approach, IEEE Trans. Ind. Electron. 56 (7) (2009) 2548–2558.
[41] W. Xie, An equivalent LMI representation of bounded real lemma for continuous-time systems, J. Inequal. Appl. 2008 (2008) 1–8.